EXAMINATION OF UAS-SFM AND UAS-LIDAR FOR SURVEY REPEATABILITY OF ROADWAY CORRIDORS

José A. Pilartes-Congo , Michael J. Starek , Mohammad Pashaei , and Jacob Berryhill

Measurement Analytics Laboratory, Conrad Blucher Institute for Surveying and Science

ABSTRACT

Uncrewed aircraft system (UAS)-based surveying offers an efficient way to produce dense point clouds of roadway corridors within the right-of-way (ROW). Common techniques include structure-from-motion and multi-view stereo (SfM/MVS) photogrammetry, or UAS-SfM, and UAS-based light detection and ranging (lidar), or UAS-Lidar. However, considerations such as measurement fidelity and postprocessing workflows are necessary to effectively deploy these technologies. This study examines UAS-SfM and UAS-Lidar survey repeatability of a roadway surface by comparing direct georeferencing solutions with and without the use of a ground control point (GCP) network. Field tests examine differences in vertical accuracy and compare differences in digital terrain model (DTM)-based change detection of roadway surface elevation. Repeat UAS-SfM and UAS-Lidar flights were conducted over a flat runway surface acting as a proxy for a typical state highway roadway corridor. The UAS-SfM surveys were conducted with a platform equipped with a 42 MP RGB digital camera and a post-processed kinematic (PPK) global navigation satellite system (GNSS) receiver for accurate image geopositioning. The UAS-Lidar surveys were conducted using a geodetic-grade RIEGL VUX-1LR long-range scanner and a Livox Avia mapping-grade scanner. Direct georeferencing solutions resulted in vertical change detection errors (i.e., root mean square errors) within 2.9 cm for UAS-SfM and between 1.6 cm and 1.8 cm for UAS-Lidar depending on the lidar sensor. The inclusion of GCPs improved UAS-SfM change detection error to within 2.3 cm while UAS-Lidar improved to 0.9 cm for the survey-grade VUX sensor and degraded to 3.1 cm for the Avia sensor.

1. INTRODUCTION

Efficient and affordable surveying workflows are important to ensure adequate conditions of right-of-way (ROW) highway corridors. While traditional surveying methods provide accurate measurements of road surface conditions, they come at the expense of tedious manual labor and exposure to unsafe situations [1]. Compared to conventional surveying techniques, uncrewed aircraft systems (UASs) can provide a costeffective and efficient means for surveying ROW corridors. When used effectively, these UAS-based methods are reliable, offer greater data coverage and density (spatial resolution), more data collection flexibility, and are less prone to safety hazards, and reduce the need to stop traffic flow [2, 3, 4].

A common UAS mapping technique uses a digital RGB camera for overlapping image acquisition and subsequent 3D reconstruction of the local scene. This technique is called structure-from-motion / multi-view stereo (SfM/MVS) photogrammetry, or UAS-SfM. Another technique relies on UAS-mounted light detection and ranging (lidar) sensors and is referred to as UAS-Lidar. Both UAS-SfM and UAS-Lidar can produce dense 3D point clouds from which derivative mapping products can be generated (e.g., 3D textured meshes and digital terrain models (DTMs)) to facilitate monitoring ROW corridors. Adequate use of UAS-SfM and UAS-Lidar requires considerations related to data collection efficiency, data accuracy, and post-processing workflows. Various studies have examined the accuracies obtainable with UAS-SfM and UAS-Lidar [5, 6, 7]. However, few studies have examined the repeatability of these survey technologies, both in accuracy and precision, for consistent monitoring of roadway surface elevation and surrounding surfaces within the ROW.

This study originates from a research project with the Texas Department of Transportation (TxDOT) focused on comparing measurement performance and workflow efficiency of UAS-SfM and UAS-Lidar to support land surveying activities. The study examines differences in UAS-SfM and UAS-Lidar for survey repeatability of exposed surfaces or roadways. The research quantifies the consistency, accuracy, and precision of roadway surface measurements and surface change detection error (i.e., root mean square error (RMSE) of the vertical component). To accomplish this goal, the study uses repeated UAS flights over a simulated roadway corridor with an established ground control point (GCP) network. UAS-SfM and UAS-Lidar flights were processed using direct georeferencing solutions with and without control.

UAS-SfM and UAS-Lidar trajectories can be processed using direct georeferencing, indirect georeferencing, or both. Direct georeferencing relies on onboard global navigation

Pilartes-Congo and Starek are also with the Department of Computer Science, College of Engineering and Computer Science, Texas A&M University-Corpus Christi (Texas, U.S.A., 78412). The authors thank the Texas Department of Transportation for partially funding this research.

satellite system (GNSS) technology to georeference UASderived products. For accurate image positioning or point cloud generation, UAS platforms should be equipped with a real-time kinematic and/or post-processed kinematic (PPK) GNSS receiver. Indirect georeferencing utilizes a ground control network (e.g., GCPs) for the same purpose. Indirect georeferencing can provide high-accuracy survey alignment to control but requires more manual labor and cannot be deployed in certain scenarios (e.g., active ROW corridors). When combining direct and indirect georeferencing, control networks are used to further constrain the direct georeferencing solutions. A major difference between UAS-SfM and UAS-Lidar trajectory corrections is that the latter requires a robust inertial navigation system (INS) with an inertial measurement unit (IMU) for obtaining sensor trajectory information. Coupling an INS with a GNSS during inertial processing of the IMU measurements allows for accurate estimation of the lidar sensor's exterior orientation.

2. METHODOLOGY

This research uses UAS data acquired over an inoperable concrete runway located at the Texas A&M University System RELLIS Campus, in Bryan, Texas, USA (Fig. 1). The area of focus measures roughly 460 m × 25 m, designed to simulate a typical state highway ROW corridor. The surveys were conducted on April 28-30, 2023 with a one-day separation.



Fig. 1: Texas A&M University System-RELLIS campus runway study site and distribution of GCPs established at the site.

The study considers a GCP network of 20 aerial panel targets distributed in a 2-1-2 staggered pattern, spaced roughly 37.5 m apart. The no-GCP assessment used all targets as checkpoints only. When conducting the 4-GCP assessments, only the four GCPs placed in the corners of the study area (yellow crosses in 1) were used to constrain the results, and the rest of the targets remained as checkpoints. The GCPs were surveyed using a Leica TS15 P 1" robotic total station

and later adjusted using the least squares adjustment tool in Carlson SurvNet (v12.0.0.13). The absolute coordinate of the network was established off a target surveyed using the Tx-DOT real-time network (RTN) based on a 3-minute average.

UAS-SfM data was obtained from a WingtraOne Gen II PPK UAS (Fig. 2a). The WingtraOne is a fixed-wing vertical take-off and landing platform equipped with a Sony RX1R II 42-megapixel RGB full-frame sensor and a PPK-enabled GNSS receiver for image trajectory correction. The camera is mounted to operate in a nadir perspective.

UAS-Lidar data was collected using a FreeFly Alta-X UAS platform equipped with either a RIEGL VUX-1LR (Fig. 2b) or a Livox Avia lidar scanner (Fig. 2c), henceforth referred to as VUX and Avia. The Alta-X is a heavy-lift rotary system designed for commercial applications. The VUX is a geodetic-grade lidar sensor that operates in the near-infrared (NIR) band (1550 nm). It has a maximum pulse rate of 820 kHz, offers up to 15 returns, uses a linear scanning mechanism with a fast-rotating mirror, and provides a field-of-view (FOV) of up to 330°. The VUX is equipped with an integrated KVH 1750 fiber optic gyroscope IMU and a dual-frequency

receiver with multia mapping-grade liband (905 nm). It up to 3 returns, and repetitive linear sca scanning pattern wi



and the sensors were deployed on two different days using said designs. Given the differences in imaging GSD of the UAS-SfM camera, which depends on ground, and differences in pulse rate, pulse energy and scan patterns of the lidar sensors, these flight designs were designed to accomplish an average point spacing of 5 cm or less across the corridor study area, thus allowing for a fairer comparison between sensors. The flight designs are summarized in Table 1. UAS trajectory corrections were aided by a locally established base station for PPK corrections using a multi-frequency Septentrio GNSS receiver. This base logged static GNSS information for a minimum of four hours. The workflow employed in this study is summarized in Fig. 3.

Platform and Sensor	Day	Altitude	Overlap	GSD	Pulse Rate	Scan FOV
Wingtra - Sony RX1R II	Day 1	120 m AGL	80% (sidelap), 80% (endlap)	1.6 cm/px	-	-
Wingtra - Sony RX1R II	Day 2	120 m AGL	80% (sidelap), 80% (endlap)	1.6 cm/px	-	-
Alta X - VUX	Day 1	80 m AGL	50% (scan overlap)	-	820 kHz	90°
Alta X - VUX	Day 2	80 m AGL	50% (scan overlap)	-	820 kHz	90°
Alta X - Avia	Day 1	60 m AGL	50% (scan overlap)	-	240 kHz	55° (linear)
Alta X - Avia	Day 2	60 m AGL	50% (scan overlap)	-	240 kHz	55° (linear)

Flowchart for IGARSS 2024 Paper



Fig. 3: Summary of workflow.

Pix4Dmatic (v1.52.1) and Spatial Explorer Pro (v7.0.8) were used to process UAS-SfM and UAS-Lidar data, respectively. A strip adjustment is an important calibration step for lidar workflows. It helps to correct systematic errors identified in 3D point cloud swath misalignment between different flight lines [8]. This optimization step performs a plane fitting of points generated from different flight lines, resulting in better-aligned 3D point clouds. In this work, strip adjustment was performed using the LiDARSnap tool in Spatial Explorer.

Roadway elevation surface change detection errors were measured based on DTMs generated from UAS-SfM and UAS-Lidar 3D point clouds. These evaluations used 30 cm DTM grids generated using the las2dem module of LAStools. This module triangulates points in a 3D point cloud into a temporary triangular irregular network (TIN) and then rasterizes the TIN onto a gridded DTM. This study then utilizes the *cloud-to-cloud distance* tool in CloudCompare (v2.12) to compute the elevation differences between Day 1 (reference dataset) and Day 2 (comparative dataset) for the different sensors. The performance of the sensors was evaluated using primarily the Δ mean_z (\overline{x}_z), Δ sigma_z (σ_z (or standard deviation)), and Δ RMSE_z metrics. Generated mapping products were referenced to the North American Datum of 1983 (2011) - State Plane Texas Central, and orthometric heights (converted from ellipsoid using GEOID18).

3. RESULTS AND DISCUSSION

Table 2 shows UAS-SfM and UAS-Lidar 3D point cloud statistics for Day 1 and Day 2. UAS-SfM provided a more consistent measure of the total number of points and density of the point cloud. These differences are explained by the different flight altitudes of the UAS-Lidar versus UAS-SfM

S-Lidar flight designs (Day 1 and Day 2).

flights and differences in imaging GSD or lidar pulse rates, platform velocity, and scan patterns. The Wingtra observed point cloud differences of 147,146 points between the two days, the VUX and Avia observed a difference of 2.17 million and 1.54 million, respectively. These discrepancies are also reflected in the average point density.

Sensor	No. of Points	Density	Spacing
Wingtra (Day 1)	6,745,482	395 pts/m ²	0.05 m
Wingtra (Day 2)	6,892,628	404 pts/m ²	0.05 m
VUX (Day 1)	6,701,591	393 pts/m ²	0.05 m
VUX (Day 2)	8,868,790	519 pts/m ²	0.04 m
Avia (Day 1)	15,936,938	934 pts/m ²	0.03 m
Avia (Day 2)	14,393,249	843 pts/m ²	0.03 m

Table 2: Point cloud statistics of UAS-SfM and UAS-Lidar.

As Fig. 4 shows, the Wingtra, VUX, and Avia obtained RMSE $_z$ values of 10-13 cm, 11-14 cm, and 6-8 cm, respectively for no-GCP cases (i.e., checkpoints only). When using 4 GCPs, the largest reduction in RMSE $_z$ occurred with the VUX (roughly 13 cm lower than the no-GCP case). This is likely due to its high degree of point cloud precision, less noise, and strong intensity values which enabled more accurate target selection, thereby helping to improve and constrain the solution.

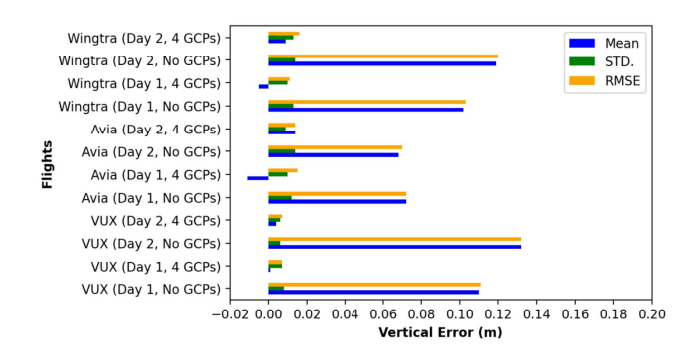


Fig. 4: Vertical errors observed with the different sensors.

Table 3 summarizes the UAS-SfM and UAS-Lidar vertical change detection error (with and without control) of the surface based on DTMs from Day 1 and Day 2. Without the use of GCPs, the following DTM difference RMSE_z

values were observed: 2.9 cm (UAS-SfM, Wingtra), 1.8 cm (UAS-Lidar, VUX), and 1.6 cm (UAS-Lidar, Avia). With four GCPs, the DTM Difference RMSE_z values were 2.3 cm (Wingtra), 0.9 cm (VUX), and 3.1 cm (Avia). This suggests an improvement for the Wingtra and VUX sensors, but not for the Avia. In addition, the table shows that the introduction of GCPs helps to remove bias or systematic errors from the solutions, thus improving the performance of the sensor and change detection errors. Fig. 5 shows the point cloud surface roughness maps for UAS-SfM and UAS-Lidar for Day 1. This map communicates differences in measurement precision along the flat runway surface. The lower standard deviation values in elevation suggest better precision in surface elevation measurement. In this regard, the VUX provides the best elevation measurement precision. This is consistent with the reduction in RMSE_z values after removing the bias.

Sensor (# of GCPs)	$\Delta \overline{x}_z$	$\Delta \sigma_z$	Δ RMSE $_z$
Wingtra (no GCPs)	0.021 m	0.020 m	0.029 m
Wingtra (4 GCPs)	0.010 m	0.021 m	0.023 m
VUX (no GCPs)	0.017 m	0.007 m	0.018 m
VUX (4 GCPs)	0.006 m	0.007 m	0.009 m
Avia (no GCPs)	0.000 m	0.016 m	0.016 m
Avia (4 GCPs)	0.026 m	0.017 m	0.031 m

Table 3: DTM differences when comparing Day 2 (comparative dataset) values against Day 1 (reference dataset).

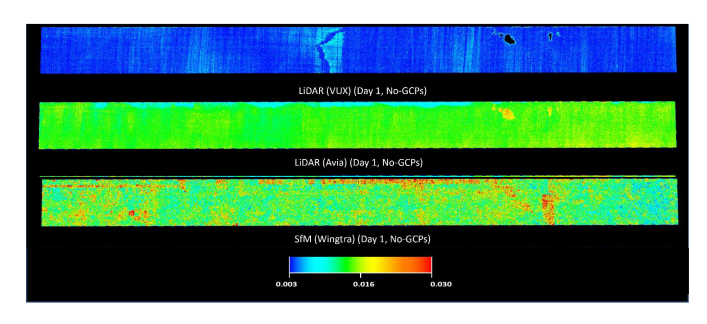


Figure: 1953/1958/Fraction of the Property of

Figure 109 summarizes the vertical accuracy results for the UAS-SfM (Wingtra) and UAS-LiDAR flights (VUX, Avia) conducted over two days at RELLIS. Accuracy results are measured relative to total station control cod din (to) Maril Jaj Sharks (GCPs). Results show vertical accuracy with, and without, use of control for unclassified point clouds due to the runway surface being exposed. Results clearly show the value in use of control for reducing vertical a Finisy stitute process mental to the cracking acting of gell ARS united (44 ARS). Lidar in repeatedly surveying ROW corridors using direct The VUXA DAR flights showed the largest reduction in Certical RMSE when using control for both and first likely due to the high regret of precision within the VUX generated point of the largest of precision within the VUX generated point of the largest of precision within the VUX generated point of the largest of precision within the VUX generated point of the largest of the largest reduction in the VUX generated point of the largest reduction in the VUX generated point of the largest reduction in the VUX generated point of the largest reduction in the VUX generated point of the largest reduction in the largest re chord atti and acRIMISES) dimit there will intensity values. The Avia LiDAR data also benefited from control as did the Wingtra data. In intensity values. The Avia Lidak data also benefited from control as did the wingtra data. In tensity refer it in the control as did the wingtra data. In tensity refer it is the control as did the wingtra data. In thr rase in precisely identifying outrol targets within the imagery. Precise target identification in LiDAR point cloud data is generally more challenging but results here show it can work well atecting/surface changes than UAS-SfM when not using GCPs. Further, GCPs improved the accuracy and reliability of both UAS-SfM and VUX-based UAS-Lidar but not Avia-based UAS-Lidar, indicating possible differences in performance between the two types of lidar sensors. Future work will

further investigate the influence of GCPs when processing the Livox Avia sensor data and explore the influence of GCP target type during UAS-Lidar strip adjustment. Further experiments will evaluate the influence of more GCP network combinations on change detection error and the impact of different GNSS trajectory correction workflows for improving survey repeatability with direct georeferencing solutions.

5. REFERENCES

- [1] Mohammad Farhadmanesh, Chandler Cross, Ali H Mashhadi, Abbas Rashidi, and Jessica Wempen, "Highway Asset and Pavement Condition Management Using Mobile Photogrammetry," *Transportation Research Record*, vol. 2675, no. 9, pp. 296–307, 2021.
- [2] Orrin Thomas, Christian Stallings, and Benjamin Wilkinson, "Unmanned Aerial Vehicles Can Accurately, Reliably, and Economically Compete with Terrestrial Mapping Methods," *Journal of Unmanned Vehicle Systems*, vol. 8, no. 1, pp. 57–74, 2019.
- [3] Stephanie R Rogers, Ian Manning, and William Livingstone, "Comparing the Spatial Accuracy of Digital Surface Models from Four Unoccupied Aerial Systems: Photogrammetry Versus LiDAR," *Remote Sensing*, vol. 12, no. 17, pp. 2806, 2020.
- [4] Suliman A. Gargoum and Karim El Basyouny, "A Literature Synthesis of LiDAR Applications in Transportation: Feature Extraction and Geometric Assessments of Highways," GIScience & Remote Sensing, vol. 56, no. 6, pp. 864–893, 2019.
- [5] Conor McMahon, Omar E. Mora, and Michael J. Starek, "Evaluating the Performance of sUAS Photogrammetry with PPK Positioning for Infrastructure Mapping," *Drones*, vol. 5, no. 2, pp. 50, 2021.
- [6] Joan-Cristian Padró, Francisco-Javier Muñoz, Jordi Planas, and Xavier Pons, "Comparison of Four UAV Georeferencing Methods for Environmental Monitoring Purposes Focusing on the Combined Use with Airborne and Satellite Remote Sensing Platforms," *International journal of applied earth observation and geoinformation*, vol. 75, pp. 130–140, 2019.
- [7] José Pilartes-Congo, Michael J Starek, and Jacob Berryhill, "Impact of Different GNSS Solutions on UAS-SfM Vertical Accuracy for Shoreline Charting," in *IGARSS* 2023-2023 IEEE International Geoscience and Remote Sensing Symposium. IEEE, 2023, pp. 4666–4669.
- [8] L. Davidson, J.P. Mills, I. Haynes, C. Augarde, P. Bryan, and M. Douglas, "Airborne to UAS LiDAR: An Analysis of UAS LiDAR Ground Control Targets," *ISPRS Geospa*tial Week 2019, 2019.